

# MgO-Doped Tantalum Coating on Ti: Microstructural Study and Biocompatibility Evaluation

Mangal Roy,<sup>†</sup> Vamsi Krishna Balla,<sup>‡</sup> Amit Bandyopadhyay,<sup>†</sup> and Susmita Bose\*,<sup>†</sup>

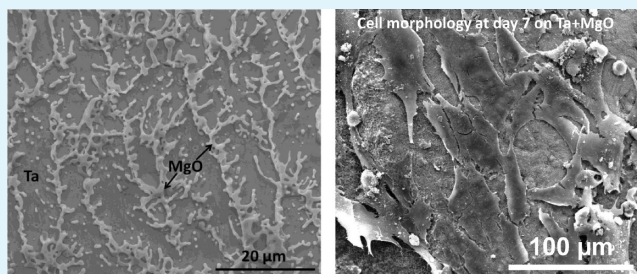
<sup>†</sup>W. M. Keck Biomedical Materials Research Laboratory, School of Mechanical and Materials Engineering, Washington State University, Pullman, Washington 99164, United States

<sup>‡</sup>Central Glass and Ceramic Research Institute, Kolkata 700032, India

## S Supporting Information

**ABSTRACT:** Pure and MgO incorporated Ta coatings were prepared on Cp-Ti substrate using laser engineered net shaping (LENS), which resulted in diffuse coating-substrate interface. MgO was found along the Ta grain boundaries in the Ta matrix that increased the coating hardness from  $185 \pm 2.7$  HV to  $794 \pm 93$  HV. *In vitro* biocompatibility study showed excellent early cellular attachment and later stage proliferation in MgO incorporated coatings. The results indicated that although Ta coatings had higher biocompatibility than Ti, it could further be improved by incorporating MgO in the coating, while simultaneously improving the mechanical properties.

**KEYWORDS:** laser processing, Ta coating, MgO coating, biocompatibility, *in vitro*



## 1. INTRODUCTION

Titanium (Ti) and its alloys are widely used for load bearing orthopedic implants because of their excellent biocompatibility and corrosion resistance. However, Ti implants are bioinert and lack desired osseointegration properties limiting their biological fixation with the bone tissues and consequent long-term *in vivo* stability.<sup>1–3</sup> Several approaches have been developed to improve bone-implant contact and overall healing process of load bearing metal implants including porous metal coatings and bioactive calcium phosphate (CaP) ceramic coatings.<sup>4,5</sup> Both approaches have shown significant promise and are currently applied to commercially available devices.<sup>2,5</sup>

Recently, tantalum (Ta) has been considered as new bioactive metal due to its excellent bioactivity and corrosion resistance.<sup>6–12</sup> Extremely high melting temperature (3017 °C), high affinity to oxygen and high manufacturing cost limits its widespread applicability. However, our recent works on laser processing of dense Ta coatings on Ti<sup>13</sup> and porous Ta structures<sup>14</sup> showed processing flexibility. Our earlier investigations on laser-processed Ta demonstrate that Ta structures present excellent biological environment for cellular adhesion, growth, and differentiation promoting early biological fixation.<sup>13–15</sup>

Several investigations show that incorporation of inorganic materials in CaP based ceramics can enhance osteoblast cell-materials interactions.<sup>16</sup> Metallic elements such as strontium (Sr), magnesium (Mg), silicon (Si), silver (Ag) have been shown to influence biological performance of CaP based ceramics.<sup>17–22</sup> Among these elements, Mg is the fourth main cation in human body and found in abundance in intracellular matrix.<sup>23</sup> It is now well-established that Mg is essential for

regulating transporters, ion channels and hundreds of enzymes and protein synthesis.<sup>24,25</sup> It also controls intracellular Ca ion concentration and pH.<sup>26</sup> It has been reported that Mg deficiency can result in reduced osteoblast number in mice and rats.<sup>23,27</sup> In some other studies, alkaline phosphatase activity, production of osteocalcin, mRNA parathyroid hormone (PTH) 1,25(OH)<sub>2</sub>-vitamin D was found to decrease in association with Mg depletion from bone.<sup>25,28,29</sup> *In vitro* studies have indicated that Mg can directly stimulate all stages of osteoblast activity.<sup>30</sup> In our earlier studies, we have shown that Mg doping in CaP ceramics can improve early stage osteoblast activity.<sup>21,22</sup> However, to the best of our knowledge, there are no reports on incorporation of MgO in metallic biomaterials and its influence on cellular activities. In the present work, we have made an attempt to create MgO doped Ta coatings using high power lasers to understand the role of MgO doping toward *in vitro* cell-materials interactions of Ta coatings on Ti. Considering the established bioactivity of Ta, comparable to that of HA, it is hypothesized that presence of MgO in the Ta coatings can potentially enhance the osteointegration properties of laser processed Ta coatings. Ta coatings with and without MgO were prepared using a Laser Engineered Net Shaping (LENS) – an additive manufacturing technique. All the coatings were characterized in terms of microstructure and *in vitro* biocompatibility using human fetal osteoblast (hFOB) cells.

Received: October 5, 2011

Accepted: January 16, 2012

Published: January 16, 2012

## 2. MATERIALS AND METHODS

**2.1. MgO-Doped Ta Coating Fabrication and Characterization.** Ta metal powder (Grandview Materials Inc., Columbus, OH) with 99.5% purity and particles size between 45 and 75  $\mu\text{m}$  was used. Ta coatings with  $\sim 1.5$  mm thickness having 10 mm diameter were deposited on 3 mm thick commercially pure (Cp) Ti plates using LENS-750 (Optomec Inc. Albuquerque, NM) equipped with a 500W continuous wave Nd:YAG laser. Detailed description of LENS operation and capabilities can be found elsewhere.<sup>31,32</sup> Dense Ta coatings were fabricated using a laser power of 450 W, a scan speed of 7 mm/s and a powder feed rate of 106 g/min.<sup>13</sup> Magnesium oxide (MgO) with 99.9995% purity (Sigma Aldrich) was mixed with 5% Polyvinyl alcohol (PVA) binder and preplaced on the laser processed Ta coatings and dried in oven at 60  $^{\circ}\text{C}$  for 24 h. The preplaced MgO powder coating was melted using LENS at 400 W with scan speed of 10 and 15 mm/s to create a Ta + MgO coatings on Ti.

To reveal microstructural features, polished Ta and Ta+MgO coating samples were further chemical polished for 30 s using a solution containing 25 mL of lactic acid, 15 mL of  $\text{HNO}_3$ , and 5 mL of HF followed by second etching with 20 mL of  $\text{HNO}_3$ , 20 mL of HF, and 60 mL of  $\text{H}_2\text{SO}_4$  solution for 60 s and observed under Field Emission Scanning Electron Microscope (FE-SEM) (FEI – Quanta 200F). Vickers microhardness measurements were made using a 300 g load for 20s ( $n = 10$ ). Constituent phases of Ta+MgO coatings were identified using a Siemens D 500 Kristalloflex diffractometer (Madison, WI, USA) with  $\text{Cu K}\alpha$  radiation.

**2.2. In vitro Biocompatibility Assessment.** All laser-processed samples in as-processed conditions were used for cell culture and MTT assay. Laser processed Ta coatings and Cp-Ti substrates were used as control. Established protocol for cell culture has been followed.<sup>17,18</sup> Cell morphology was determined after 3 and 7 days of culture using human osteoblast cell line hFOB 1.19 (ATCC, Manassas, VA) cells. Cell proliferation was determined by MTT assay after 3, 7, and 11 days of culture. Statistical analysis was performed using Student's  $t$  test, and  $p < 0.05$  ( $n = 3$ ) was considered statistically significant.

## 3. RESULTS AND DISCUSSION

### 3.1. Microstructure, Hardness, and Phase Analysis.

During laser processing, the interaction between laser beam and powder depends on the incident laser energy, as well as on the physical properties of powder used. In general, increasing the laser power, decreasing the scan speed and decreasing the powder feed rate increases the specific laser energy input enabling fabrication of dense coatings/parts. In the present work, we have used 400 W laser power with a scan speed for 10 and 15 mm/s to melt the preplaced MgO on Ta coatings. At these conditions, considerable amount of burning/evaporation of MgO was observed during laser melting. Since the melting temperature of Ta is around 3017  $^{\circ}\text{C}$  a high energy input is required to completely melt the Ta coating, while ensuring good bonding between the MgO coating and Ta coating.

Our earlier investigations<sup>33,34</sup> show that the presence of secondary materials in the metal during laser processing can increase the laser absorptivity. As a result, the peak melt pool temperatures are expected to exceed the melting temperatures of metal matrix (3017  $^{\circ}\text{C}$  for Ta in the present work) and can reach temperatures as high as 3500  $^{\circ}\text{C}$ . Such a high melt pool temperatures can melt and even evaporate fine fraction of MgO particles (melting point: 2830  $^{\circ}\text{C}$ ; boiling point: 3600  $^{\circ}\text{C}$ ) in the present coatings. However, the MgO coatings processed at 10 and 15 mm/s scan speed showed distinct MgO particles in the coatings primarily along the Ta grain boundaries in the remelted region of the coatings. However, the severity of burning/evaporation was found to be relatively high in the coatings processed at 10 mm/s compared to 15 mm/s.

Increasing the scan speed to 15 mm/s resulted in improvement in the MgO incorporation in the remelted region. As shown in Figure 1a, the coatings processed at 10 mm/s showed relatively

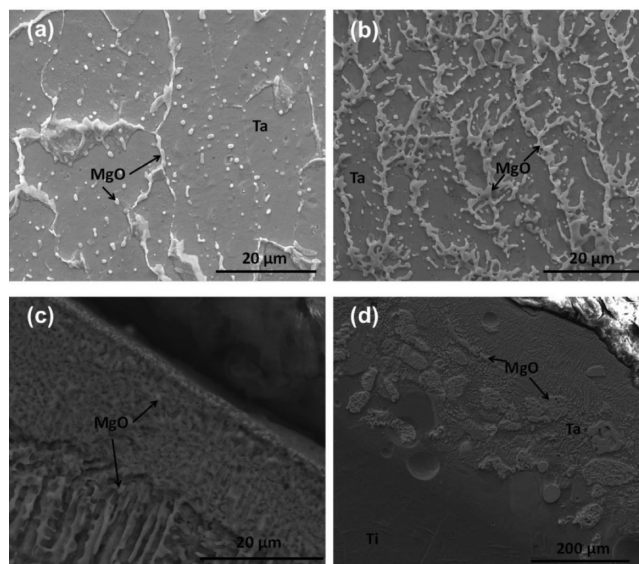


**Figure 1.** Cross-sectional SEM microstructures of MgO coated Ta coatings processed at 400 W: (a) 10 mm/s, (b–d) 15 mm/s.

small amount of MgO compared to the coatings deposited at 15 mm/s (Figure 1b–d). High scan speeds decreased the heat input to the laser beam-materials interaction zone reducing the peak melt pool temperatures, which significantly decreased the burning/evaporation of MgO powder. Since the coatings processed at 15 mm/s showed relatively high amount of MgO retention further testing and biological characterization was carried out on those samples only.

The X-ray diffraction results of laser processed MgO coatings on Ta are shown in Figure 2. In spite of burning/evaporation of

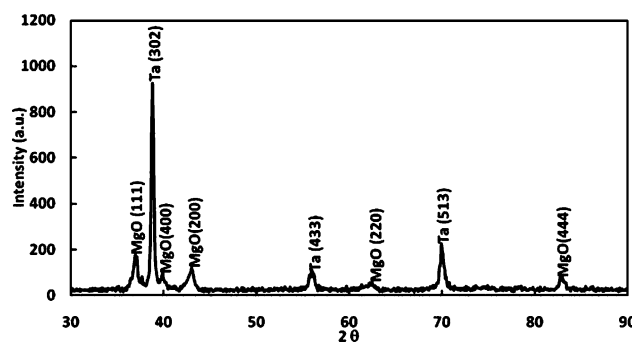


**Figure 2.** X-ray diffraction results of MgO coatings on Ta processed at 400 W and 15 mm/s.

the MgO during laser processing, the XRD results clearly demonstrated that the coatings retained measurable amount of MgO. The retention of MgO in the Ta coatings was further substantiated by the hardness measurements on these coatings. The hardness increased to  $794 \pm 93$  HV in Ta+MgO coating compared to base Ti hardness of  $185 \pm 2.7$  HV. The hardness of composite region was also higher than the hardness of Ta coatings without MgO ( $296 \pm 31$  HV). The increase in hardness of Ta+MgO coatings is due to the strengthening effect of MgO particles, which act as dislocation pinning sites during



deformation of matrix. Large variation in the hardness can be attributed to the variations in concentration and distribution of MgO particles in the coatings. The high hardness of Ta+MgO coatings compared to Ta coatings can potentially minimize the early stage bone-implant interface micromotion induced wear debris generation and associated implant loosening.<sup>35</sup>

**3.2. In vitro Biocompatibility.** hFOB cell proliferation on the coated samples was determined using MTT assay at 3, 7, and 11 days of culture and the results are shown in Figure 3.

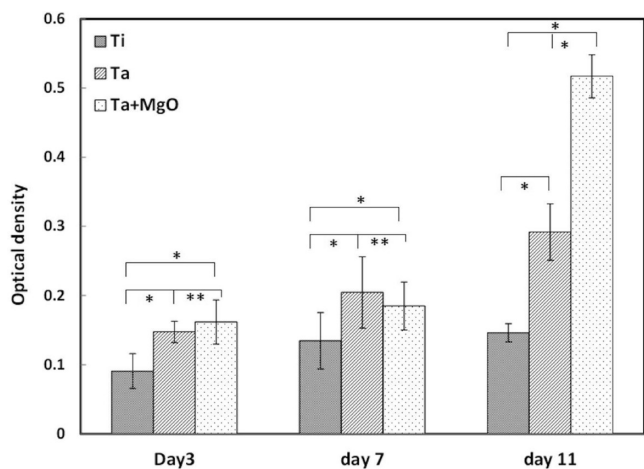


**Figure 3.** Optical density measurement illustrating hFOB cell proliferation on Ti, Ta coating, and Ta+MgO coating after 3, 7, and 11 days of culture (\* $p < 0.05$  and \*\* $p > 0.05$ ,  $n = 3$ ).

Higher cell density was observed on both Ta and Ta+MgO coatings compared to Ti control throughout the experiment. Effect of MgO in cell proliferation was not found at early time points and only realized at 11 days of culture.

Cellular attachment and growth of the hFOB cells on the control Ti, Ta coatings and Ta+MgO coatings were analyzed by FESEM. Figure 4 shows the cellular morphology and

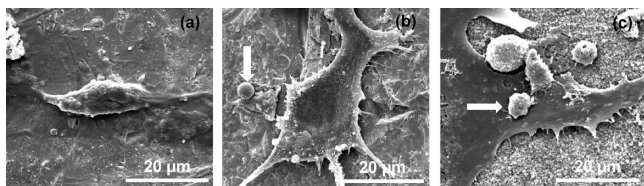


**Figure 4.** FE-SEM micrographs illustrating the hFOB cell morphologies after 3 days of culture: (a) Ti, (b) Ta coatings, (c) Ta + MgO coatings. The spherical objects in (b, indicated by white arrow) are Ta particles and that of c are apatite nodules.

attachment behavior on uncoated and coated surfaces after 3 days of culture. As noted in Figure 4a, hFOB cells on the control Ti surface show only few filopodia extensions indicating inadequate cellular attachment and spreading. Comparatively, cells on the Ta surfaces had a flattened morphology with larger cellular microextensions, as can be seen in Figure 4b. Similar to Ta coatings, hFOB cells exhibited the phenotypic expressions on Ta+MgO coatings, however, with greater surface coverage, as shown in Figure 4c. Figure 5 shows the cellular morphology after 7 days of culture. Cells grew in numbers and spread well to cover both Ta and Ta+MgO surfaces. hFOB cells reached near confluence on the coated surfaces and therefore any morphological differences were not noticed in these samples. In

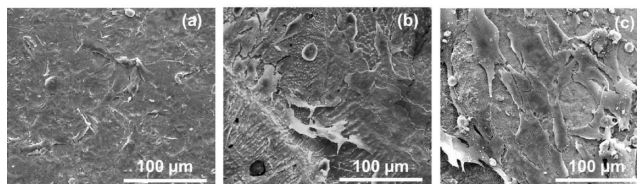


**Figure 5.** FE-SEM micrographs illustrating the hFOB cell morphologies after 7 days of culture: (a) Ti, (b) Ta coatings, (c) Ta + MgO coatings.

comparison to coated surfaces, cells did not reach confluence on control Ti surface (Figure 5a).

The success and desired performance of orthopedic implants are largely dependent on the cellular activity at the implant surface. Orthopedic implant surface chemistry plays an important role in osteoblast adhesion, proliferation and subsequent differentiation.<sup>18,22</sup> Osteoblast cells use integrins as signal transduction and adhesive proteins to attach to a substrate surface. It has been shown that presence of Mg in bioceramics can significantly increase the expression of  $\beta 1$ ,  $\alpha 5\beta 1$ , and  $\alpha 3\beta 1$  integrins, which are essential for osteoblast activity.<sup>36,37</sup> Along with integrins, other key signaling proteins, such as Shc (Src homology collagen), focal adhesion kinase, and collagen type 1 are also highly expressed by osteoblast cells in presence of Mg.<sup>38</sup> The flattened morphology of the hFOB cells at day 3 on the Ta+MgO coating surface with numerous cellular microextensions indicate a better adhesion which can be attributed to the presence of Mg in the coating.<sup>18,21</sup> After adhesion, the osteoblast cells proliferate on the implant surface before differentiation and biomineralization. At day 7 we see higher number of cells covering both the coating surfaces which is in line with recent publications indicating that Ta surface with or without MgO provide a suitable surface for cell proliferation.<sup>13,14</sup> However, due to the presence of MgO in the coating, hFOB cells proliferate rapidly at later stage of the culture. The phenomenon can be explained in many ways. Among several factors, melastatin-like transient receptor potential 7 (TRPM7), which is also known as Mg ion channel, plays an important role in osteoblast proliferation and survival.<sup>39</sup> TRPM7 channels are also responsible for intracellular Mg ion homeostasis in osteoblast cells. Presence of Mg in the Ta+MgO coatings help in up regulating these ion channels and facilitate osteoblast cell proliferation compared to pure Ta coatings. Moreover, intracellular Mg ion controls intracellular Ca ion concentration that controls cell proliferation and secretion.<sup>26</sup> The multifunctional role of Mg results in higher cell density on Ta+MgO coatings at day 11. In summary, incorporation of MgO in laser processed Ta coatings is proven beneficial to improve not only mechanical properties, but also facilitates osteoblast activity. Further studies will be focused on determining the biocompatibility of the coatings with matured osteoblasts and its ability to support differentiation of mesenchymal stem cells into matured bone cells.

#### 4. CONCLUSIONS

Using LENS, we have successfully deposited pure and MgO incorporated Ta coatings on Cp-Ti substrate. The structural incorporation of MgO in Ta matrix resulted in a 4-fold increase in coating hardness compared to Cp-Ti. In vitro biocompatibility study indicated superior biocompatibility of Ta coatings compared to uncoated Ti which was further improved by incorporating MgO in the Ta coatings. Good initial adhesion of

hFOB cells and increased later stage proliferation was noticed due to MgO incorporation in Ta coatings compared to pure Ta coatings. The results indicated that LENS processing of Ta +MgO coatings can improve both mechanical and biological properties simultaneously.

## ■ ASSOCIATED CONTENT

### Supporting Information

Materials, methods, and characterization information regarding cell culture. This material is available free of charge via the Internet at <http://pubs.acs.org>.

## ■ AUTHOR INFORMATION

### Corresponding Author

\*Tel: 509-335-7461. Fax: 509-335-4662. E-mail: [sbose@wsu.edu](mailto:sbose@wsu.edu).

## ■ ACKNOWLEDGMENTS

The authors acknowledge the financial support from National Institutes of Health (Grant NIH-R01-EB-007351), M. J. Murdock Charitable Trust, and National Science Foundation (NSF). The authors also acknowledge the financial support from the W. M. Keck Foundation to establish a Biomedical Materials Research Lab at WSU.

## ■ REFERENCES

- (1) Das, K.; Bose, S.; Bandyopadhyay, A. *Acta Biomater.* **2007**, *3*, 573–585.
- (2) Mäkelä, K. T.; Eskelinen, A.; Pulkkinen, P.; Paavolainen, P.; Remes, V. *J. Bone Jt. Surg., Am. Vol.* **2008**, *90*, 2160–2170.
- (3) Chambers, B.; Clair, S. F.; Froimson, M. I. *J. Arthroplasty* **2007**, *22* (s1), 71–74.
- (4) Narayanan, R.; Seshadri, S. K.; Kwon, T. Y.; Kim, K. H. *J. Biomed. Mater. Res.* **2008**, *85B*, 279–299.
- (5) Wazen, R. M.; Lefebvre, L. P.; Baril, E.; Nanci, A. *J. Biomed. Mater. Res.* **2010**, *94B*, 64–71.
- (6) Kato, H.; Nakamura, T.; Nishiguchi, S.; Matsusue, Y.; Kobayashi, M.; Miyazaki, T.; Kim, H. M.; Kokubo, T. *J. Biomed. Mater. Res.* **2000**, *53*, 28–35.
- (7) Bobyn, J. D.; Stackpool, G. J.; Hacking, S. A.; Tanzer, M.; Krygier, J. J. *J. Bone Jt. Surg., Br. Vol.* **1999**, *81B*, 907–914.
- (8) Hacking, S. A.; Bobyn, J. D.; Toh, K.; Tanzer, M.; Krygier, J. J. *J. Biomed. Mater. Res.* **2000**, *52*, 631–638.
- (9) Matsuno, H.; Yokoyama, A.; Watari, F.; Motohiro, U.; Kawasaki, T. *Biomaterials* **2001**, *22*, 1253–1262.
- (10) Miyazaki, T.; Kim, H. M.; Kokubo, T.; Ohtsuki, C.; Kato, H.; Nakamura, T. *Biomaterials* **2002**, *23*, 827–832.
- (11) Kokubo, T.; Kim, H. M.; Kawashita, M. *Biomaterials* **2003**, *24*, 2161–2175.
- (12) Balla, V. K.; Bose, S.; Davies, N. M.; Bandyopadhyay, A. *JOM* **2010**, *62*, 61–64.
- (13) Balla, V. K.; Banerjee, S.; Bose, S.; Bandyopadhyay, A. *Acta Biomater.* **2010**, *6*, 2329–2334.
- (14) Balla, V. K.; Bodhak, S.; Bose, S.; Bandyopadhyay, A. *Acta Biomater.* **2010**, *6*, 3349–3359.
- (15) Roy, M.; Balla, V. K.; Bandyopadhyay, A.; Bose, S. *Adv. Eng. Mater. (Adv. Biomater.)* **2010**, *12*, B637–B641.
- (16) Boanini, E.; Gazzano, M.; Bigi, A. *Acta Biomater.* **2010**, *6*, 1882–1894.
- (17) Bose, S.; Tarafder, S.; Banerjee, S. S.; Davies, N. M.; Bandyopadhyay, A. *Bone* **2011**, *48*, 1282–1290.
- (18) Roy, M.; Bandyopadhyay, A.; Bose, S. *J. Biomed. Mater. Res., Part B – Appl. Biomater* **2011**, *99B*, 258–265.
- (19) Banerjee, S. S.; Tarafder, M. S.; Davies, N. M.; Bandyopadhyay, A.; Bose, S. *Acta Biomater.* **2010**, *6*, 167–174.

- (20) Hoppe, A.; Güldal, N. S.; Boccaccini, A. R. *Biomaterials* **2011**, *32*, 2757–2774.
- (21) Xue, W.; Dahlquist, K.; Banerjee, A.; Bandyopadhyay, A.; Bose, S. *J. Mater. Sci. Mater. Med.* **2008**, *19*, 2669–2677.
- (22) Bandyopadhyay, A.; Bernard, S.; Xue, W.; Bose, S. *J. Am. Ceram. Soc.* **2006**, *89*, 2675–2688.
- (23) Rude, R. K.; Singer, F. R.; Gruber, H. E. *J. Am. Coll. Nutr.* **2009**, *28*, 131–141.
- (24) Schmitz, C.; Deason, F.; Perraud, A. L. *Magnes. Res.* **2007**, *20*, 6–18.
- (25) Abed, E.; Moreau, R. *Am. J. Physiol. Cell Physiol.* **2009**, *297*, C360–C368.
- (26) Zhang, A.; Cheng, T. P.; Altura, B. M. *Biochim. Biophys. Acta* **1992**, *1134*, 25–29.
- (27) Rude, R. K.; Gruber, H. E. *J. Nutr. Biochem.* **2004**, *15*, 710–716.
- (28) Creedon, A.; Flynn, A.; Cashman, K. Br. *J. Nutr.* **1999**, *82*, 63–71.
- (29) Rude, R. K.; Gruber, H. E.; Norton, H. J.; Wei, L. Y.; Frausto, A.; Kilburn, J. *Bone* **2005**, *37*, 211–219.
- (30) Liu, C. C.; Yeh, J. K.; Aloia, J. F. *J. Bone Miner. Res.* **1988**, *3*, S104.
- (31) Roy, M.; Balla, V. K.; Bandyopadhyay, A.; Bose, S. *Acta Biomater.* **2008**, *4*, 324–333.
- (32) Roy, M.; Bandyopadhyay, A.; Bose, S. *Mater. Sci. Eng., C* **2009**, *29*, 1965–1968.
- (33) Das, M.; Balla, V. K.; Basu, D.; Bose, S.; Bandyopadhyay, A. *Scr. Mater.* **2010**, *63*, 438–441.
- (34) Das, M.; Bysakh, S.; Basu, D.; Sampathkumar, T. S.; Balla, V. K.; Bose, S.; Bandyopadhyay, A. *Surf. Coat. Technol.* **2011**, *205*, 4366–4373.
- (35) Ditttrick, S.; Balla, V. K.; Bose, S.; Bandyopadhyay, A. *Mater. Sci. Eng., C* **2011**, *31*, 1832–1835.
- (36) Zreiqat, H.; Howlett, C. R.; Zannettino, A.; Evans, P.; Schulze-Tanzil, G.; Knabe, C.; Shakibaei, M. *J. Biomed. Mater. Res. B.* **2002**, *62*, 175–184.
- (37) Gronthos, S.; Stewart, K.; Graves, S. E.; Hay, S.; Simmons, P. J. *J. Bone Miner. Res.* **1997**, *12*, 1189–1197.
- (38) Schlaepfer, D. D.; Hanks, S. K.; Hunter, T.; Van-der-Geer, P. *Nature* **1994**, *372*, 786–791.
- (39) Nadler, M. J.; Hermosura, M. C.; Inabe, K.; Perraud, A. L.; Zhu, Q.; Stokes, A. J.; Kurosaki, T.; Kinet, J. P.; Penner, R.; Scharenberg, A. M.; Fleig, A. *Nature* **2001**, *411*, 590–595.